Nucl. Phys. B 1015 (2025) 116904

Contents lists available at ScienceDirect

Nuclear Physics, Section B

journal homepage: www.elsevier.com/locate/nuclphysb

Particle Cosmology

Barrow holographic dark energy with varying exponent

Spyros Basilakos [a,b,c], Andreas Lymperis [d,*], Maria Petronikolou [a,e], Emmanuel N. Saridakis [a,f,g]

[a] National Observatory of Athens, Lofos Nymfon, 11852 Athens, Greece
[b] Academy of Athens, Research Center for Astronomy and Applied Mathematics, Soranou Efesiou 4, 11527, Athens, Greece
[c] School of Sciences, European University Cyprus, Diogenes Street, Engomi, 1516 Nicosia, Cyprus
[d] Department of Physics, University of Patras, 26500 Patras, Greece
[e] Department of Physics, National Technical University of Athens, Zografou Campus GR 157 73, Athens, Greece
[f] Department of Astronomy, School of Physical Sciences, University of Science and Technology of China, Hefei 230026, PR China
[g] Departamento de Matemáticas, Universidad Católica del Norte, Avda. Angamos 0610, Casilla 1280 Antofagasta, Chile

ARTICLE INFO

Editor: Yasaman Farzan

ABSTRACT

We construct Barrow holographic dark energy with varying exponent. Such an energy-scale-dependent behavior is typical in quantum field theory and quantum gravity under renormalization group considerations, however in the present scenario it has an additional justification, since in realistic cases one expects that Barrow entropy quantum-gravitational effects to be stronger at early times and to smooth out and disappear at late times. We impose specific, redshift-dependent ansätze for the Barrow running exponent, such as the linear, CPL-like, exponential, and trigonometric ones, and we investigate their cosmological behavior. We show that we can recover the standard thermal history of the universe, with the sequence of matter and dark energy epochs, in which the transition from deceleration to acceleration happens at $z \approx 0.65$, in agreement with observations. In the most realistic case of hyperbolic tangent ansatz, in which we can easily bound Barrow exponent inside its theoretically determined bounds 0 and 1 for all redshifts, we see that the dark-energy equation-of-state parameter can be quintessence like, or experience the phantom-divide crossing, while in the future it can either tend to the cosmological constant value or start increasing again. All these features reveal that Barrow holographic dark energy with varying exponent is not only theoretically more justified than the standard, constant-exponent case, but it leads to richer cosmological behavior too.

Contents

1. Introduction . . . 2
2. Standard Barrow holographic dark energy . . . 2
3. Barrow holographic dark energy with varying exponent . . . 4
4. Cosmological evolution . . . 4
   4.1. Linear case . . . 5
   4.2. CPL-like case . . . 5

* Corresponding author.
E-mail addresses: svasil@academyofathens.gr (S. Basilakos), alymperis@upatras.gr (A. Lymperis), petronikoloumaria@mail.ntua.gr (M. Petronikolou), msaridak@noa.gr (E.N. Saridakis).

https://doi.org/10.1016/j.nuclphysb.2025.116904
Received 16 July 2024; Received in revised form 4 April 2025; Accepted 6 April 2025

Available online 8 April 2025

4.3. Exponential case . . . 6
4.4. Hyperbolic tangent case . . . 7
4.5. Trigonometric functions case . . . 9
5. Conclusions . . . 10
Declaration of competing interest . . . 11
Acknowledgements . . . 11
Data availability . . . 11
References . . . 11

1. Introduction

The progression from the matter era to the accelerated expansion phase in the late universe is now a well-established phenomenon. While the cosmological constant is the simplest explanation, challenges related to its quantum-field-theoretical calculation and the possibility of a dynamical nature have prompted two primary approaches to construct extended scenarios. The first retains general relativity as the underlying gravitational theory and introduces the concept of dark energy [1–3] as the acceleration source. The second involves constructing extended gravity theories which provide the required richer structure [4–7].

An alternative explanation for the origin of dark energy emerges through the cosmological application of the holographic principle [8–10]. This framework, rooted in the thermodynamics of black holes, connects the ultraviolet cutoff of a quantum field theory with the largest distance of the theory, a prerequisite for its applicability at large distances [11]. In a region where entropy is proportional to volume, the total energy should not exceed the mass of a black hole with the same radius, and this saturation leads to the extraction of a holographically originated vacuum energy, and thus to a form of holographic dark energy with a dynamic nature [12,13]. The cosmological implications of holographic dark energy are intriguing [12–22] and align with observations [23–28]. Additionally, one has the advantage that holographic scenarios are free from potential pathologies that may appear in modified gravity [7]. Hence, holographic dark energy has spurred extensive research, leading to various extensions [29–60].

One large class of holographic dark energy extension is obtained by changing the underlying entropy relation. In particular, the base models use the standard Bekenstein-Hawking entropy. However, since there are many extended entropies, that arise through various considerations, such as Tsallis non-additive entropy [61], Barrow quantum-gravity corrected entropy [62], Kaniadakis relativistic entropy [63,64], power-law corrected entropy [65,66] etc, one can respectively obtain Tsallis holographic dark energy [67,68], Barrow holographic dark energy [69–71], Kaniadakis holographic dark energy [72,73], power-law holographic dark energy [74], etc.

All the above extended-entropy scenarios incorporate a constant parameter that quantifies the deviation form standard entropy. However, in principle one expects a dynamical, energy-scale-dependent behavior for this parameter, aligning with the typical case observed in quantum field theory and quantum gravity under renormalization group applications. In particular, all parameters and coupling constants demonstrate a running nature in tandem with the energy scale, and in a cosmological framework this would effectively generate a time-dependence. A first investigation of Tsallis holographic dark energy models with extended entropy with varying exponent was performed in [75] and it was shown that the running behavior can lead to interesting physical implications.

Nevertheless, in the case of Barrow entropy one has an additional necessity for the varying behavior. Since it arises from quantum-gravitational phenomena on the horizon structure, parametrized by the single exponent Δ [62], where $\Delta = 0$ corresponds to standard entropy and $\Delta = 1$ to maximal deviation, it is hard to justify why in the recent Universe one has significant quantum-gravitational phenomena in its horizon that could lead to significant deviation from standard, i.e. classical entropy. Hence, it is more natural to consider that at early times these quantum phenomena are more intense and thus Δ is closer to 1, while as time passes they smooth out and Δ tends to its standard value 0. We mention here that such a scenario is still Barrow entropy, since Δ does arise from quantum gravitational phenomena, however one goes beyond the first approximation of [62] in which these phenomena are constant throughout the Universe evolution, and examines more realistic scenarios in which quantum gravitational phenomena are stronger at early times and smooth out as the system becomes larger. In summary, a scenario of Barrow entropy with varying exponent has even more justification than the usual energy-scale dependence of coupling constants.

Since Barrow entropy has been shown to lead to a very interesting cosmological phenomenology, in the present work we are interested in studying Barrow holographic dark energy with varying exponent. In particular, we impose various parametrizations for the time-dependence, which is equivalent to redshift-dependence, and we examine their effect on the cosmological evolution. The plan of the work is the following. In Section 2 we review standard Barrow holographic dark energy, and then in Section 3 we construct the extended scenario where the Barrow exponent is varying. In Section 4 we impose specific ansätze for the Barrow running exponent and we investigate their cosmological behavior. Finally, in Section 5 we summarize our results.

2. Standard Barrow holographic dark energy

In this section we briefly review the scenario of Barrow holographic dark energy following [69]. Barrow entropy is given by [62]

$$S_B = \left(\frac{A}{A_0}\right)^{1+\Delta/2}, \tag{2.1}$$

where A is the standard horizon area and A_0 the Planck area, while the exponent Δ quantifies the quantum-gravitational deformation. Incorporating (2.1) in the definition of the standard holographic dark energy, expressed as the inequality $\rho_{DE}L^4 \leq S$, with L the horizon length, and imposing that $S \propto A \propto L^2$ [13] will result in

$$\rho_{DE} = CL^{\Delta-2}, \tag{2.2}$$

with C a parameter with dimensions $[L]^{-2-\Delta}$. In case where $\Delta = 0$, expression (2.2) recovers standard holographic dark energy $\rho_{DE} = 3c^2M_p^2L^{-2}$ (here M_p is the Planck mass), where $C = 3c^2M_p^2$ and c^2 the model parameter.

We focus on a flat homogeneous and isotropic Friedmann-Robertson-Walker (FRW) geometry with metric

$$ds^2 = -dt^2 + a^2(t)\delta_{ij}dx^i dx^j\,, \tag{2.3}$$

where $a(t)$ is the scale factor. Furthermore, we consider that the universe is filled with the matter perfect fluid, as well as with the Barrow holographic dark energy [69]

$$\rho_{DE} = CR_h^{\Delta-2}, \tag{2.4}$$

where the horizon length L in (2.2) is substituted by the future event horizon R_h [12], given by

$$R_h \equiv a\int_t^\infty \frac{dt}{a} = a\int_a^\infty \frac{da}{Ha^2}, \tag{2.5}$$

with $H \equiv \dot{a}/a$ the Hubble parameter. We then obtain the two Friedmann equations

$$3M_p^2H^2 = \rho_m + \rho_{DE} \tag{2.6}$$

$$-2M_p^2\dot{H} = \rho_m + p_m + \rho_{DE} + p_{DE}, \tag{2.7}$$

with ρ_m and p_m the energy density and pressure of matter and p_{DE} the pressure of Barrow holographic dark energy.

The matter sector is conserved, namely it satisfies the continuity equation $\dot{\rho}_m + 3H(\rho_m + p_m) = 0$. Considering matter to be dust, namely imposing $p_m = 0$, leads to $\rho_m = \rho_{m0}/a^3$, with ρ_{m0} the present matter energy density, i.e. at $a_0 = 1$ (in the following the subscript "0" denotes the value of the corresponding quantity at present). Finally, we focus on physically interesting observables such as the density parameters

$$\Omega_m \equiv \frac{1}{3M_p^2H^2}\rho_m \tag{2.8}$$

$$\Omega_{DE} \equiv \frac{1}{3M_p^2H^2}\rho_{DE}, \tag{2.9}$$

as well as on the effective dark-energy equation-of-state parameter

$$w_{DE} \equiv \frac{p_{DE}}{\rho_{DE}}. \tag{2.10}$$

Combining the aforementioned density parameters with equations (2.4) and (2.5), leads to [69]

$$\int_x^\infty \frac{dx}{Ha} = \frac{1}{a}\left(\frac{C}{3M_p^2H^2\Omega_{DE}}\right)^{\frac{1}{2-\Delta}}, \tag{2.11}$$

with $x \equiv \ln a$. Additionally, substituting $\rho_m = \rho_{m0}/a^3$ into (2.8), results to $\Omega_m = \Omega_{m0}H_0^2/(a^3H^2)$, from which, using the Friedmann equation $\Omega_m + \Omega_{DE} = 1$, we obtain

$$\frac{1}{Ha} = \frac{\sqrt{a(1-\Omega_{DE})}}{H_0\sqrt{\Omega_{m0}}}. \tag{2.12}$$

Inserting (2.12) into equation (2.11) we acquire the expression

$$\int_x^\infty \frac{dx}{H_0\sqrt{\Omega_{m0}}}\sqrt{a(1-\Omega_{DE})} = \frac{1}{a}\left(\frac{C}{3M_p^2H^2\Omega_{DE}}\right)^{\frac{1}{2-\Delta}}. \tag{2.13}$$

Taking the derivative of (2.13) with respect to $x = \ln a$ results to

$$\frac{\Omega'_{DE}}{\Omega_{DE}(1-\Omega_{DE})} = \Delta + 1 + Q(1-\Omega_{DE})^{\frac{\Delta}{2(\Delta-2)}}(\Omega_{DE})^{\frac{1}{2-\Delta}}e^{\frac{3\Delta}{2(\Delta-2)}x}, \tag{2.14}$$

with

$$Q \equiv (2-\Delta)\left(\frac{C}{3M_p^2}\right)^{\frac{1}{\Delta-2}}\left(H_0\sqrt{\Omega_{m0}}\right)^{\frac{\Delta}{2-\Delta}}, \tag{2.15}$$

and where primes denote derivatives with respect to x. This is the differential equation determining the evolution of Barrow holographic dark energy, whose solution provides Ω_{DE}. Finally, since from (2.4) we acquire $\dot{\rho}_{DE} = (\Delta-2)CR_h^{\Delta-3}\dot{R}_h$, with $\dot{R}_h$ calculated using (2.5) as $\dot{R}_h = HR_h - 1$, and since $\dot{\rho}_{DE} + 3H(\rho_{DE} + p_{DE}) = 0$, using (2.14) we finally extract [69]

$$w_{DE} = -\frac{1+\Delta}{3} - \frac{Q}{3}(\Omega_{DE})^{\frac{1}{2-\Delta}}(1-\Omega_{DE})^{\frac{\Delta}{2(\Delta-2)}}e^{\frac{3\Delta}{2(2-\Delta)}x}. \tag{2.16}$$

All the above expressions, for $\Delta = 0$ recover standard holographic dark energy with $w_{DE}|_{\Delta=0} = -\frac{1}{3} - \frac{2}{3}\sqrt{\frac{3M_p^2\Omega_{DE}}{C}}$ [12,13]. The scenario of Barrow holographic dark energy has interesting cosmological implications, and has been studied in detail in the literature [69,71,76–92].

3. Barrow holographic dark energy with varying exponent

In this section we will investigate the cosmological scenario of Barrow holographic dark energy with varying exponent Δ, namely we consider that $\Delta \equiv \Delta(x)$. In this case, the analysis of the previous section remains the same up to (2.13). However, taking its derivative requires to consider also the derivative of Δ, which will yield Δ' terms in the equations. In particular, differentiating (2.13) with respect to $x \equiv \ln a$, leads to

$$\frac{\Omega'_{DE}}{\Omega_{DE}(1-\Omega_{DE})} = \sqrt{\Omega_{DE}}\left(\frac{C}{3M_p^2}\right)^{-\frac{1}{2}}\left[\frac{P(1-\Omega_{DE})}{\Omega_{DE}}\right]^{\frac{\Delta}{2(\Delta-2)}}(2-\Delta) + \Delta + 1 + \log\left[\frac{P(1-\Omega_{DE})}{\Omega_{DE}}\right]^{\frac{\Delta'}{\Delta-2}}, \tag{3.1}$$

with

$$P = P(x) \equiv \frac{Ce^{3x}}{3M_p^2H_0^2\Omega_{m0}}. \tag{3.2}$$

Equation (3.1) is the one that determines the evolution of Barrow holographic dark energy for dust matter in a flat universe, where primes denote derivatives with respect to x.

Additionally, let us calculate the equation-of-state parameter w_{DE} for this general scenario. We differentiate (2.4), which leads to $\dot{\rho}_{DE} = CR_h^{\Delta-2}\left[\log R_h\,\dot{\Delta} + \frac{\dot{R}_h(\Delta-2)}{R_h}\right]$, with $\dot{R}_h = HR_h - 1$. Taking into account the dark energy conservation equation $\dot{\rho}_{DE} + 3H\rho_{DE}(1+w_{DE}) = 0$ and the aforementioned relations, we result to

$$(\Delta-2)C\left(\frac{\rho_{DE}}{C}\right)^{\frac{\Delta-3}{\Delta-2}}\left[H\left(\frac{\rho_{DE}}{C}\right)^{\frac{1}{\Delta-2}} - 1\right] + \rho_{DE}\dot{\Delta}\log\left(\frac{\rho_{DE}}{C}\right)^{\frac{1}{\Delta-2}} + 3H\rho_{DE}(1+w_{DE}) = 0. \tag{3.3}$$

Hence, inserting H from (2.12), and using (2.9) we finally obtain

$$w_{DE} = -\frac{\Delta+1}{3} + \frac{(\Delta-2)\sqrt{\Omega_{DE}}}{3}\left(\frac{C}{3M_p^2}\right)^{-\frac{1}{2}}\left[\frac{P(1-\Omega_{DE})}{\Omega_{DE}}\right]^{\frac{\Delta}{2(\Delta-2)}} - \frac{\Delta'}{3}\log\left[\frac{P(1-\Omega_{DE})}{\Omega_{DE}}\right]^{\frac{1}{2-\Delta}}. \tag{3.4}$$

In the case where $\Delta = const.$ we recover equation (2.16) of the previous section.

4. Cosmological evolution

In the previous section we extracted the necessary cosmological equations, which can describe the evolution in the scenario at hand. In order to investigate in detail the cosmological behavior, in what follows it is more convenient to use the redshift z instead of x through the relation $x \equiv \ln a = -\ln(1+z)$. Hence, the derivative of a function f in terms of x easily becomes derivative in terms of z through $f' = -(1+z)\frac{df}{dz}$.

We will consider several ansätze for the Barrow running exponent, which will be given by the general expression $\Delta(z) = \alpha + \beta f(z)$, where α, β are constants and $f(z)$ a function of the redshift parameter z. Nevertheless, we impose that the exponent Δ acquires values away from the standard 0-value at early times, while as time passes it tends closer to the standard value $\Delta = 0$.

We mention here that we parameterize the way that quantum gravitational phenomena smooth out, i.e. Δ as a function of redshift, in a purely phenomenological manner, through various functions. Definitely each of these functions at the fundamental level should correspond to a particular way that quantum gravitational phenomena behave.

Since the differential equation (3.1) cannot be solved analytically, we will elaborate it numerically. For initial conditions we impose $\Omega_{DE}(x=-\ln(1+z)=0)\equiv\Omega_{DE0}\approx 0.7$ and therefore $\Omega_m(x=-\ln(1+z)=0)\equiv\Omega_{m0}\approx 0.3$ in agreement with observations [93].

4.1. Linear case

As a first example, let us consider the linear ansatz $\Delta(z)=\alpha+\beta z$. Inserting it into equation (3.1) we acquire

$$\frac{-(1+z)}{\Omega_{DE}\left(1-\Omega_{DE}\right)}\frac{d\Omega_{DE}}{dz}=\sqrt{\Omega_{DE}}\left(\frac{C}{3M_p^2}\right)^{-\frac{1}{2}}\left[\frac{P(1-\Omega_{DE})}{\Omega_{DE}}\right]^{\frac{\alpha+\beta z}{2(\alpha+\beta z-2)}}(2-\alpha-\beta z)$$
$$+\log\left[\frac{P(1-\Omega_{DE})}{\Omega_{DE}}\right]^{\frac{-\beta(1+z)}{\alpha+\beta z-2}}+\alpha+\beta z+1, \tag{4.1}$$

and consequently equation (3.4) becomes

$$w_{DE}=-\frac{\alpha+\beta z+1}{3}+\frac{(\alpha+\beta z-2)\sqrt{\Omega_{DE}}}{3}\left(\frac{C}{3M_p^2}\right)^{-\frac{1}{2}}\left[\frac{P(1-\Omega_{DE})}{\Omega_{DE}}\right]^{\frac{\alpha+\beta z}{2(\alpha+\beta z-2)}}$$
$$+\frac{(1+z)\beta}{3}\log\left[\frac{P(1-\Omega_{DE})}{\Omega_{DE}}\right]^{\frac{1}{2-\alpha-\beta z}}. \tag{4.2}$$

In the upper graph of Fig. 1, we depict the evolution of the dark energy and matter density parameters in terms of redshift. As we can see, we acquire the usual thermal history of the universe, with the sequence of matter and dark energy epochs, and in the far future, namely at $z\to -1$, the universe results asymptotically to a complete dark energy dominated phase. Furthermore, in the middle graph we depict the evolution of the dark energy equation-of-state parameter, which is determined by (4.2). As we observe, the value of w_{DE} at present is around -1 in agreement with observations, lying in the quintessence regime, while in the future it asymptotically goes to the cosmological constant value. Lastly, in the lower graph we depict the deceleration parameter

$$q\equiv -1-\frac{\dot{H}}{H^2}=\frac{1}{2}+\frac{3}{2}w_{DE}\Omega_{DE}. \tag{4.3}$$

We can see the transition from deceleration to acceleration at $z\approx 0.65$, in agreement with observational data. Note that, as required, the parameter β should be suitably smaller than α in order for Δ to remain between 0 and 1. However, since there will be always a z in which this will not be the case, it is clear that this ansatz is valid only at small redshifts. Hence, in the following we proceed to the investigation of ansätze with full applicability.

4.2. CPL-like case

Inspired by the Chevallier-Polarski-Linder (CPL) parameterization for the dark-energy equation of state [94,95], we consider a varying exponent of the form $\Delta(z)=\alpha+\frac{\beta z}{z+1}$, which can always be less than 1 for arbitrarily large redshifts. In this case substituting into (3.1) we obtain

$$\frac{-(1+z)}{\Omega_{DE}\left(1-\Omega_{DE}\right)}\frac{d\Omega_{DE}}{dz}=\sqrt{\Omega_{DE}}\left(\frac{C}{3M_p^2}\right)^{-\frac{1}{2}}\left[\frac{P(1-\Omega_{DE})}{\Omega_{DE}}\right]^{\frac{\alpha(z+1)+\beta z}{2(\alpha-2)(z+1)+2\beta z}}\left[2-\alpha-\frac{\beta z}{z+1}\right]$$
$$+\log\left[\frac{P(1-\Omega_{DE})}{\Omega_{DE}}\right]^{-\frac{\beta}{(\alpha-2)(z+1)+\beta z}}+\alpha+\frac{\beta z}{z+1}+1, \tag{4.4}$$

while equation (3.4) gives

$$w_{DE}=-\frac{\alpha+\frac{\beta z}{z+1}+1}{3}+\frac{\left(\alpha+\frac{\beta z}{z+1}-2\right)\sqrt{\Omega_{DE}}}{3}\left(\frac{C}{3M_p^2}\right)^{-\frac{1}{2}}\left[\frac{P(1-\Omega_{DE})}{\Omega_{DE}}\right]^{\frac{\alpha(z+1)+\beta z}{2(\alpha-2)(z+1)+2\beta z}}$$
$$-\frac{\beta}{3(z+1)}\log\left[\frac{P(1-\Omega_{DE})}{\Omega_{DE}}\right]^{\frac{z+1}{(2-\alpha)(z+1)-\beta z}}. \tag{4.5}$$

The behavior of dark energy and matter density parameters, of the deceleration parameter, and of the dark-energy equation-of-state parameter, is similar to the one of the linear case. Nevertheless, although very efficient in describing the past Universe evolution, the CPL-like parametrization is not suitable for the future evolution, since the Barrow exponent will become larger than 1 or smaller than 0, and hence in the following we investigate more realistic cases.

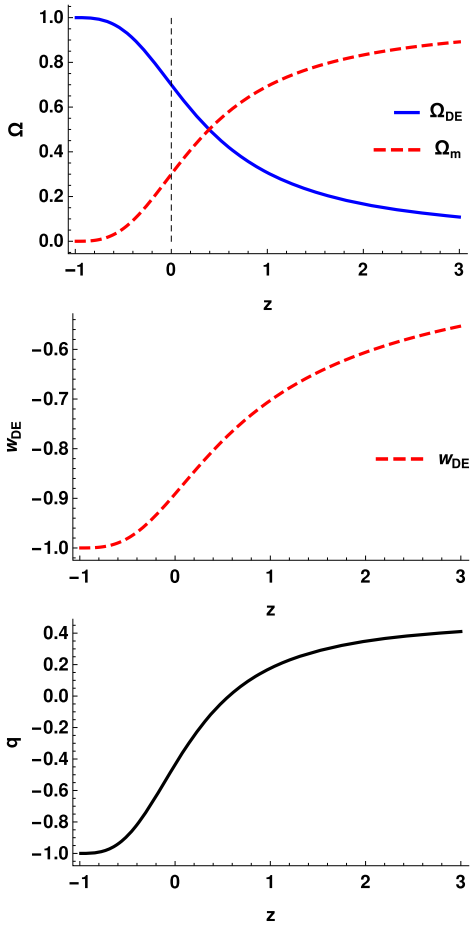

Fig. 1. Barrow holographic dark energy in the linear case where $\Delta(z) = \alpha + \beta z$. **Upper graph**: The dark energy density parameter Ω_{DE} (blue-solid) and the matter density parameter Ω_m (red-dashed), as a function of the redshift z, for $C = 1$ and $\alpha = 10^{-3}$, $\beta = 10^{-4}$, in units where $M_p^2 = 1$. **Middle graph**: The corresponding dark energy equation-of-state parameter w_{DE}. **Lower graph**: The corresponding deceleration parameter q. In all graphs we have set $\Omega_{DE}(x = -\ln(1+z) = 0) \equiv \Omega_{DE0} \approx 0.7$, in agreement with observations.

4.3. Exponential case

One ansatz that can be suitable for all redshifts is the exponential one, namely $\Delta(z) = \alpha + \beta e^{-\lambda z}$, where λ is a constant. In this case substituting into (3.1) we obtain

$$\frac{-(1+z)}{\Omega_{DE}\left(1-\Omega_{DE}\right)}\frac{d\Omega_{DE}}{dz} = \sqrt{\Omega_{DE}}\left(\frac{C}{3M_p^2}\right)^{-\frac{1}{2}}\left[\frac{P(1-\Omega_{DE})}{\Omega_{DE}}\right]^{\frac{\alpha+\beta e^{-\lambda z}}{2(\alpha+\beta e^{-\lambda z}-2)}}[2-(\alpha+\beta e^{-\lambda z})]$$
$$+\log\left[\frac{P(1-\Omega_{DE})}{\Omega_{DE}}\right]^{\frac{(1+z)\beta\lambda e^{-\lambda z}}{\alpha+\beta e^{-\lambda z}-2}} + \alpha + \beta e^{-\lambda z} + 1, \tag{4.6}$$

while equation (3.4) gives

$$w_{DE} = -\frac{\alpha+\beta e^{-\lambda z}+1}{3} + \frac{(\alpha+\beta e^{-\lambda z}-2)\sqrt{\Omega_{DE}}}{3}\left(\frac{C}{3M_p^2}\right)^{-\frac{1}{2}}\left[\frac{P(1-\Omega_{DE})}{\Omega_{DE}}\right]^{\frac{\alpha+\beta e^{-\lambda z}}{2(\alpha+\beta e^{-\lambda z}-2)}}$$
$$-\frac{(1+z)\beta\lambda e^{-\lambda z}}{3}\log\left[\frac{P(1-\Omega_{DE})}{\Omega_{DE}}\right]^{\frac{1}{2-\alpha-\beta e^{-\lambda z}}}. \tag{4.7}$$

Fig. 2 shows the evolution of the dark energy and matter density parameters, and similarly to the linear case we acquire the usual thermal history of the universe. Additionally, from the middle graph we observe that w_{DE} lies in the quintessence regime and its present value is around -1 according to observations. Finally, in the lower graph we depict the deceleration parameter q, where the transition from deceleration to acceleration in this case happens at $z \approx 0.65$.

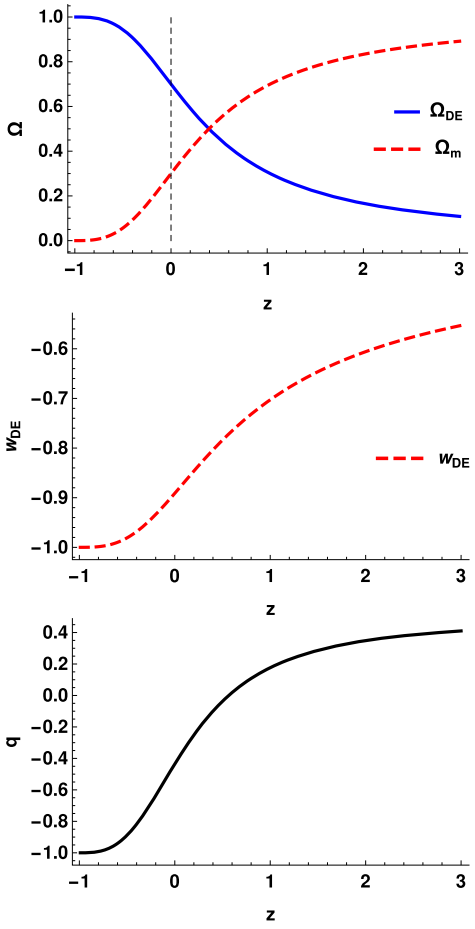

Fig. 2. Barrow holographic dark energy in the exponential case with $\Delta(z) = \alpha + \beta e^{-\lambda z}$. **Upper graph**: The dark energy density parameter Ω_{DE} (blue-solid) and the matter density parameter Ω_m (red-dashed), as a function of the redshift z, for $C = 1$ and $\alpha = 10^{-3}$, $\beta = 10^{-4}$, $\lambda = 5 \cdot 10^{-5}$, in units where $M_p^2 = 1$. **Middle graph**: The corresponding dark energy equation-of-state parameter w_{DE}. **Lower graph**: The corresponding deceleration parameter q. In all graphs we have set $\Omega_{DE}(x = -\ln(1+z) = 0) \equiv \Omega_{DE0} \approx 0.7$, in agreement with observations.

4.4. Hyperbolic tangent case

One ansatz that can be very suitable for the purpose of Barrow holographic dark energy with varying exponent is the hyperbolic tangent one, since in this case we can immediately bound Δ between 0 and 1 for all redshifts, obtaining easily a case where $\Delta(z)$ is 1 at early times while it becomes 0 at intermediate and late times, as well as in the future.

We consider the form $\Delta(z) = \alpha + \beta \tanh(\gamma z)$. Inserting into equation (3.1) yields

$$\frac{-(1+z)}{\Omega_{DE}\left(1-\Omega_{DE}\right)}\frac{d\Omega_{DE}}{dz} = \sqrt{\Omega_{DE}}\left(\frac{C}{3M_p^2}\right)^{-\frac{1}{2}}\left[\frac{P(1-\Omega_{DE})}{\Omega_{DE}}\right]^{\frac{\alpha+\beta\tanh(\gamma z)}{2[\alpha+\beta\tanh(\gamma z)-2)]}}[2-\alpha-\beta\tanh(\gamma z)]$$
$$+\log\left[\frac{P(1-\Omega_{DE})}{\Omega_{DE}}\right]^{\frac{-(1+z)\beta\gamma\,\mathrm{sech}^2(\gamma z)}{\alpha+\beta\tanh(\gamma z)-2}} + \alpha + \beta\tanh(\gamma z) + 1, \tag{4.8}$$

and

$$w_{DE} = \frac{[\alpha+\beta\tanh(\gamma z)-2]\sqrt{\Omega_{DE}}}{3}\left(\frac{C}{3M_p^2}\right)^{-\frac{1}{2}}\left[\frac{P(1-\Omega_{DE})}{\Omega_{DE}}\right]^{\frac{\alpha+\beta\tanh(\gamma z)}{2[\alpha+\beta\tanh(\gamma z)-2)]}}$$
$$-\frac{\alpha+\beta\tanh(\gamma z)+1}{3}+\frac{(1+z)\beta\gamma\,\mathrm{sech}^2(\gamma z)}{3}\log\left[\frac{P(1-\Omega_{DE})}{\Omega_{DE}}\right]^{\frac{1}{2-\alpha-\beta\tanh\gamma z}}. \tag{4.9}$$

In the following we set $\alpha = \beta = \frac{1}{2}$ which fixes the largest value of $\Delta(z)$ to 1 and the smallest to 0, in consistency with Barrow entropy. Hence the only model parameter is γ, which determines how fast the transition from 1 to 0 takes place.

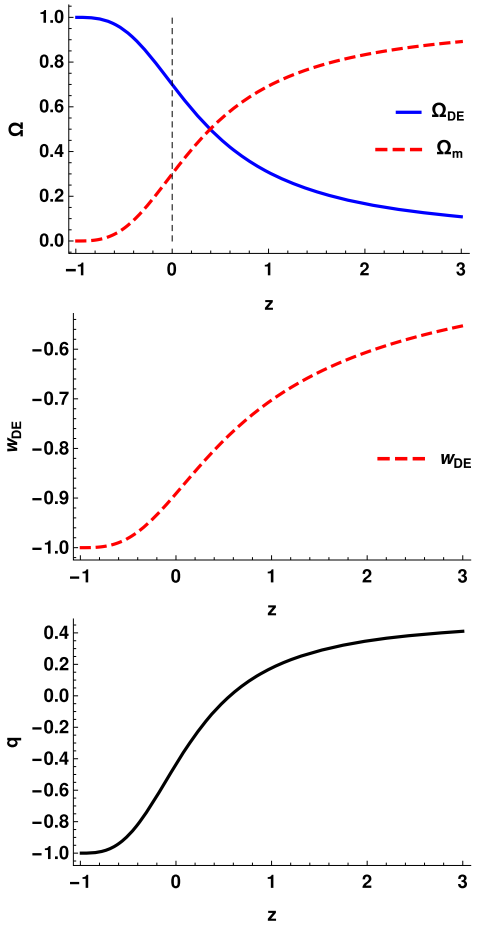

Fig. 3. Barrow holographic dark energy in the Hyperbolic Tangent case with $\Delta(z) = \alpha + \beta \tanh(\gamma z)$, for $\alpha = \beta = \frac{1}{2}$. **Upper graph**: The dark energy density parameter Ω_{DE} (blue-solid) and the matter density parameter Ω_m (red-dashed), as a function of the redshift z, for $C = 1$ and $\gamma = 0.001$, in units where $M_p^2 = 1$. **Middle graph**: The corresponding dark energy equation-of-state parameter w_{DE}. **Lower graph**: The corresponding deceleration parameter q. In all graphs we have set $\Omega_{DE}(x = -\ln(1+z) = 0) \equiv \Omega_{DE0} \approx 0.7$, in agreement with observations.

In the upper graph of Fig. 3 we depict the behavior of the dark energy and matter density parameters. As we can see, we acquire the sequence of matter and dark energy epochs, and in the far future the universe results asymptotically to a complete dark-energy dominated phase. Furthermore, the dark energy equation-of-state parameter, in this specific example lies in the quintessence regime, while at present times and in the future it is around -1. Lastly, the deceleration parameter q experiences the transition from deceleration to acceleration at around $z \approx 0.65$.

Since the hyperbolic tangent form is the most realistic case, we explore it further. In particular, we are interested in examining what is the effect of the single parameter γ on the dark-energy equation-of-state parameter. In Fig. 4, we depict the evolution of w_{DE}, for various values of the γ. A general observation is that for increasing γ the value of w_{DE} decreases. Additionally, one can see that for some cases it can experience the phantom-divide crossing. Interestingly enough, in the future w_{DE} can either tend to -1 or even start increasing again. These features reveals the capabilities of the model, and the advantages of Barrow holographic dark energy with running exponent comparing to standard Barrow holographic dark energy.

We close this subsection by confronting the model of the hyperbolic tangent case at hand with Supernovae type Ia (SNIa) and Cosmic Chronometer data. For SNIa, it is well established that the relation between the apparent and absolute magnitudes follows

$$2.5 \log \left[\frac{L}{l(z)} \right] = \mu \equiv m(z) - M = 5 \log \left[\frac{d_L(z)_{\rm obs}}{M\, pc} \right] + 25 \,, \tag{4.10}$$

with $l(z)$ and $m(z)$ the apparent luminosity and apparent magnitude, and L and M the absolute luminosity and magnitude, respectively, while $d_L(z)_{\rm obs}$ is the luminosity distance. Moreover, the theoretical expression for the luminosity distance is given by

$$d_L(z)_{\rm th} \equiv (1+z) \int_0^z \frac{dz'}{H(z')} \,. \tag{4.11}$$

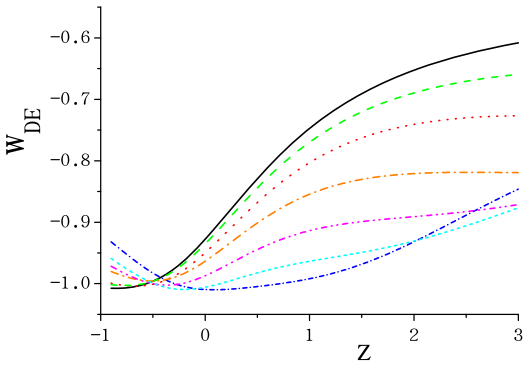

Fig. 4. The evolution of the dark-energy equation-of-state parameter for Barrow holographic dark energy in the Hyperbolic Tangent case with $\Delta(z) = \alpha + \beta \tanh(\gamma z)$, for $\alpha = \beta = \frac{1}{2}$. The various curves correspond to $\gamma = 0.01$ (black solid), $\gamma = 0.05$ (green dashed), $\gamma = 0.1$ (red dotted), $\gamma = 0.2$ (orange dashed-dotted), $\gamma = 0.3$ (magenta dashed-dotted-dotted), $\gamma = 0.4$ (cyan short-dashed), and $\gamma = 0.5$ (blue short dashed-dotted), in units where $M_p^2 = 1$. In all cases we have imposed $\Omega_{DE}(x = -\ln(1+z) = 0) \equiv \Omega_{DE0} \approx 0.7$ at present, in agreement with observations.

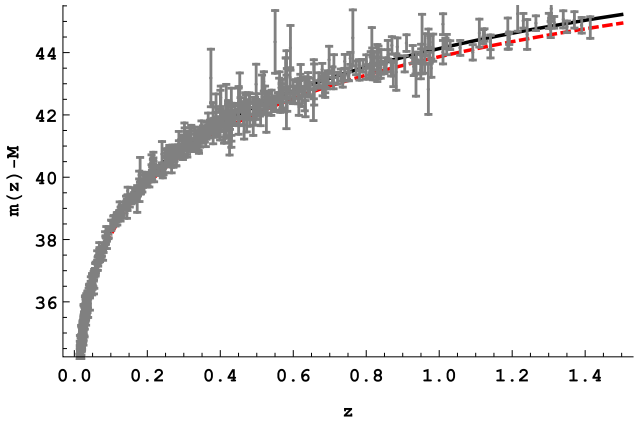

Fig. 5. The apparent minus absolute magnitude predicted theoretically in the Hyperbolic Tangent case (red - dashed) with $\alpha = \beta = 1/2$ and with $\gamma = 0.001$, in units where $M_p^2 = 1$, on top of the Pantheon SNIa data points from [96]. For comparison we depict the ΛCDM curve (black - solid) too.

Since the hyperbolic tangent case, as well as the ΛCDM scenario, provide predictions for $H(z)$, we compare the theoretically computed apparent minus absolute magnitudes with the binned Pantheon SNIa data from [96] in Fig. 5. As illustrated, the agreement is very good, with our model accurately reproducing the observed cosmological behavior.

In addition, the Cosmic Chronometer (CC) dataset, based on the measurement of $H(z)$ from the relative ages of passively evolving galaxies, allows us to compare the observed $H(z)$ values with our model predictions. In Fig. 6, we show the comparison between the theoretical evolution of $H(z)$ in our model with a hyperbolic tangent form and the ΛCDM model with the CC data points from [97], presented at a 2σ confidence level. The agreement is again very good, with our model reproducing the observed accelerating expansion for the parameter set $\{\alpha, \beta, \gamma\} = \{0.5, 0.5, 0.001\}$.

In summary, there exist regions in the parameter space of our model that are able to reproduce the observed evolution of the Hubble function. This suggests that this model is a viable candidate. A more thorough evaluation, including likelihood analysis and model selection using complete cosmological datasets, will be presented in future work.

4.5. Trigonometric functions case

Finally, inspired by the oscillatory parametrizations of the dark-energy equation-of-state parameters [98], one could think of richer cases, where the Barrow exponent oscillates around a mean positive value close to 0. One such case could be the $\Delta(z) = \alpha + \beta \sin z$ with $0 < \beta < \alpha$, which leads to

$$\frac{-(1+z)\Omega'_{DE}}{\Omega_{DE}\left(1-\Omega_{DE}\right)} = \sqrt{\Omega_{DE}}\left(\frac{C}{3M_p^2}\right)^{-\frac{1}{2}}\left[\frac{P(1-\Omega_{DE})}{\Omega_{DE}}\right]^{\frac{\alpha+\beta\sin z}{2(\alpha+\beta\sin z-2)}}(2-\alpha-\beta\sin z)$$
$$+\log\left[\frac{P(1-\Omega_{DE})}{\Omega_{DE}}\right]^{\frac{-(1+z)\beta\cos z}{\alpha+\beta\sin z-2}}+\alpha+\beta\sin z+1, \tag{4.12}$$

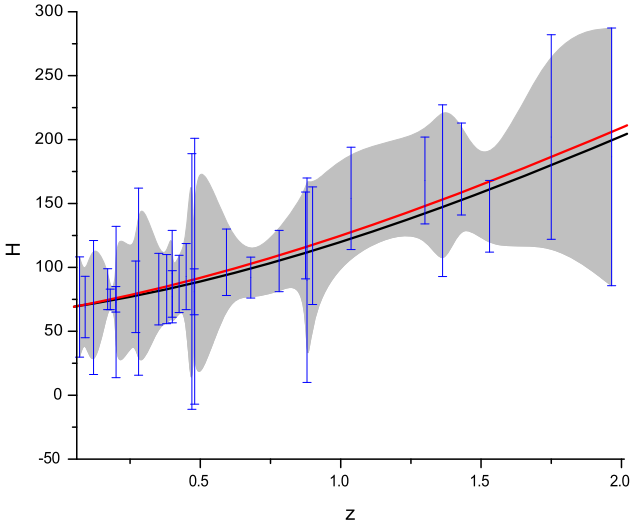

Fig. 6. The Hubble parameter $H(z)$ in units of Km/s/Mpc as a function of the redshift, for the hyperbolic tangent case with $\alpha = \beta = 1/2$ and with $\gamma = 0.001$ (red-solid), in $M_p^2 = 1$ units, on top of the Cosmic Chronometers data points from [97] at 2σ confidence level. For comparison we depict the ΛCDM curve (black - solid) too. We have imposed $\Omega_{m0} \approx 0.31$.

$$w_{DE} = -\frac{\alpha+\beta\sin z+1}{3} + \frac{(\alpha+\beta\sin z-2)\sqrt{\Omega_{DE}}}{3}\left(\frac{C}{3M_p^2}\right)^{-\frac{1}{2}}\left[\frac{P(1-\Omega_{DE})}{\Omega_{DE}}\right]^{\frac{\alpha+\beta\sin z}{2(\alpha+\beta\sin z-2)}}$$
$$+\frac{(1+z)\beta\cos z}{3}\log\left[\frac{P(1-\Omega_{DE})}{\Omega_{DE}}\right]^{\frac{1}{2-\alpha-\beta\sin z}}. \tag{4.13}$$

Alternatively, one could consider $\Delta(z) = \alpha + \beta\cos z$, obtaining

$$\frac{-(1+z)\Omega'_{DE}}{\Omega_{DE}\left(1-\Omega_{DE}\right)} = \sqrt{\Omega_{DE}}\left(\frac{C}{3M_p^2}\right)^{-\frac{1}{2}}\left[\frac{P(1-\Omega_{DE})}{\Omega_{DE}}\right]^{\frac{\alpha+\beta\cos z}{2(\alpha+\beta\cos z-2)}}(2-\alpha-\beta\cos z)$$
$$+\log\left[\frac{P(1-\Omega_{DE})}{\Omega_{DE}}\right]^{\frac{(1+z)\beta\sin z}{\alpha+\beta\cos z-2}} + \alpha+\beta\cos z+1, \tag{4.14}$$

$$w_{DE} = -\frac{\alpha+\beta\cos z+1}{3} + \frac{(\alpha+\beta\cos z-2)\sqrt{\Omega_{DE}}}{3}\left(\frac{C}{3M_p^2}\right)^{-\frac{1}{2}}\left[\frac{P(1-\Omega_{DE})}{\Omega_{DE}}\right]^{\frac{\alpha+\beta\cos z}{2(\alpha+\beta\cos z-2)}}$$
$$-\frac{(1+z)\beta\sin z}{3}\log\left[\frac{P(1-\Omega_{DE})}{\Omega_{DE}}\right]^{\frac{1}{2-\alpha-\beta\cos z}} \tag{4.15}$$

The behavior of dark energy and matter density parameters, of the deceleration parameter, and of the dark-energy equation-of-state parameter, is similar to the one of the previous models.

5. Conclusions

In this work we constructed Barrow holographic dark energy with varying exponent. This scenario is an extension of holographic dark energy with Barrow entropy, where the involved Barrow exponent, which quantifies the deviation from standard Bekenstein-Hawking entropy, is allowed to present a running behavior. Such an energy-scale-dependent behavior is typical in quantum field theory and quantum gravity under renormalization group considerations, however in the present scenario it has an additional justification, if not necessity, since in realistic cases one expects that Barrow entropy quantum-gravitational effects to be stronger at early times and to smooth out and disappear at late times. Hence, in the cosmological framework of an expanding Universe, this would effectively generate Barrow-exponent with time-dependence.

After constructing the extended scenario we imposed specific ansätze for the Barrow running exponent and we investigated their cosmological behavior. We started with the linear case, where we showed that we can recover the standard thermal history of the universe, with the sequence of matter and dark energy epochs. Additionally, we saw that the dark-energy equation-of-state parameter w_{DE} lies in the quintessence regime and tends to -1 in the future, where the universe results asymptotically to a complete dark energy dominated phase. Finally, from the behavior of the deceleration parameter we saw that the transition from deceleration to acceleration happens at $z \approx 0.65$, in agreement with observations.

The linear ansatz is suitable only for small redshifts, since there will be always a redshift in which the Barrow exponent could exceed the theoretically determined bounds. The CPL-like ansatz is applicable at all redshifts in the past, however is still not suitable for the future evolution. Hence, we proceeded to the examination of a more realistic case, namely the exponential ansatz. In this model, we obtained a similar behavior, with a sequence of matter and dark-energy epochs and the transition to acceleration at $z \approx 0.65$ too.

Nevertheless, the most suitable ansatz for the purpose of Barrow holographic dark energy with varying exponent is the hyperbolic tangent one, since in this case we can easily bound Barrow exponent between 0 and 1 for all redshifts, obtaining a scenario where $\Delta(z)$ is 1 at early times while it becomes 0 at intermediate and late times, as well as in the future. This scenario can also recover the thermal history of the Universe, and the recent transition to acceleration. Furthermore, we investigated the effect of the single parameter γ on the dark-energy equation-of-state parameter. We showed that for increasing γ the value of w_{DE} decreases, while for some cases it can experience the phantom-divide crossing, and that in the future w_{DE} can either tend to -1 or start increasing again. For completeness, we performed a basic confrontation of the hyperbolic tangent model against the Supernovae type Ia (SnIa) and Cosmic Chronometers (CC) datasets, as a first evidence that they are viable and consistent with observations. Lastly, we also presented the case where the running Barrow exponent has a trigonometric form.

All these features reveal that Barrow holographic dark energy with varying exponent is not only theoretically more justified than the standard, constant-exponent case, but it leads to richer cosmological behavior too. It would be interesting to perform a full observational confrontation with data from Supernovae type Ia (SNIa), Baryonic Acoustic Oscillations (BAO), Cosmic Microwave Background (CMB), and Cosmic Chronometers (CC) probes, in order to construct the likelihood contours and extract constraints on the involved parameters, and apply information criteria in order to compare the scenario with the concordance ΛCDM cosmology. Such a full observational analysis is left for a future project.

Declaration of competing interest

The authors declare that they have no known competing financial interests or personal relationships that could have appeared to influence the work reported in this paper.

Acknowledgements

M.P. is supported by the Basic Research program of the National Technical University of Athens (NTUA, PEVE) 65232600-ACT-MTG: Alleviating Cosmological Tensions Through Modified Theories of Gravity. The authors acknowledge the contribution of the LISA CosWG and of the COST Action CA21136 “Addressing observational tensions in cosmology with systematics and fundamental physics (CosmoVerse)”.

Data availability

No data was used for the research described in the article.

References

[1] E.J. Copeland, M. Sami, S. Tsujikawa, Dynamics of dark energy, Int. J. Mod. Phys. D 15 (2006) 1753, arXiv:hep-th/0603057.
[2] Y.-F. Cai, E.N. Saridakis, M.R. Setare, J.-Q. Xia, Quintom cosmology: theoretical implications and observations, Phys. Rep. 493 (2010) 1, arXiv:0909.2776.
[3] K. Bamba, S. Capozziello, S. Nojiri, S.D. Odintsov, Dark energy cosmology: the equivalent description via different theoretical models and cosmography tests, Astrophys. Space Sci. 342 (2012) 155, arXiv:1205.3421.
[4] S. Nojiri, S.D. Odintsov, Unified cosmic history in modified gravity: from F(R) theory to Lorentz non-invariant models, Phys. Rep. 505 (2011) 59, arXiv:1011.0544.
[5] S. Capozziello, M. De Laurentis, Extended theories of gravity, Phys. Rep. 509 (2011) 167, arXiv:1108.6266.
[6] Y.-F. Cai, S. Capozziello, M. De Laurentis, E.N. Saridakis, f(T) teleparallel gravity and cosmology, Rep. Prog. Phys. 79 (2016) 106901, arXiv:1511.07586.
[7] CANTATA collaboration, Y. Akrami, et al., Modified Gravity and Cosmology: An Update by the CANTATA Network, Springer, 2021, arXiv:2105.12582.
[8] W. Fischler, L. Susskind, Holography and cosmology, arXiv:hep-th/9806039.
[9] D. Bak, S.-J. Rey, Cosmic holography, Class. Quantum Gravity 17 (2000) L83, arXiv:hep-th/9902173.
[10] P. Horava, D. Minic, Probable values of the cosmological constant in a holographic theory, Phys. Rev. Lett. 85 (2000) 1610, arXiv:hep-th/0001145.
[11] A.G. Cohen, D.B. Kaplan, A.E. Nelson, Effective field theory, black holes, and the cosmological constant, Phys. Rev. Lett. 82 (1999) 4971, arXiv:hep-th/9803132.
[12] M. Li, A model of holographic dark energy, Phys. Lett. B 603 (2004) 1, arXiv:hep-th/0403127.
[13] S. Wang, Y. Wang, M. Li, Holographic dark energy, Phys. Rep. 696 (2017) 1, arXiv:1612.00345.
[14] R. Horvat, Holography and variable cosmological constant, Phys. Rev. D 70 (2004) 087301, arXiv:astro-ph/0404204.
[15] Q.-G. Huang, M. Li, The holographic dark energy in a non-flat universe, J. Cosmol. Astropart. Phys. 08 (2004) 013, arXiv:astro-ph/0404229.
[16] D. Pavon, W. Zimdahl, Holographic dark energy and cosmic coincidence, Phys. Lett. B 628 (2005) 206, arXiv:gr-qc/0505020.
[17] B. Wang, Y.-g. Gong, E. Abdalla, Transition of the dark energy equation of state in an interacting holographic dark energy model, Phys. Lett. B 624 (2005) 141, arXiv:hep-th/0506069.
[18] S. Nojiri, S.D. Odintsov, Unifying phantom inflation with late-time acceleration: scalar phantom-non-phantom transition model and generalized holographic dark energy, Gen. Relativ. Gravit. 38 (2006) 1285, arXiv:hep-th/0506212.
[19] H. Kim, H.W. Lee, Y.S. Myung, Equation of state for an interacting holographic dark energy model, Phys. Lett. B 632 (2006) 605, arXiv:gr-qc/0509040.
[20] B. Wang, C.-Y. Lin, E. Abdalla, Constraints on the interacting holographic dark energy model, Phys. Lett. B 637 (2006) 357, arXiv:hep-th/0509107.
[21] M.R. Setare, Interacting holographic dark energy model in non-flat universe, Phys. Lett. B 642 (2006) 1, arXiv:hep-th/0609069.
[22] M.R. Setare, E.N. Saridakis, Non-minimally coupled canonical, phantom and quintom models of holographic dark energy, Phys. Lett. B 671 (2009) 331, arXiv:0810.0645.
[23] X. Zhang, F.-Q. Wu, Constraints on holographic dark energy from Type Ia supernova observations, Phys. Rev. D 72 (2005) 043524, arXiv:astro-ph/0506310.

[24] M. Li, X.-D. Li, S. Wang, X. Zhang, Holographic dark energy models: a comparison from the latest observational data, J. Cosmol. Astropart. Phys. 06 (2009) 036, arXiv:0904.0928.
[25] C. Feng, B. Wang, Y. Gong, R.-K. Su, Testing the viability of the interacting holographic dark energy model by using combined observational constraints, J. Cosmol. Astropart. Phys. 09 (2007) 005, arXiv:0706.4033.
[26] X. Zhang, Holographic Ricci dark energy: current observational constraints, quintom feature, and the reconstruction of scalar-field dark energy, Phys. Rev. D 79 (2009) 103509, arXiv:0901.2262.
[27] J. Lu, E.N. Saridakis, M.R. Setare, L. Xu, Observational constraints on holographic dark energy with varying gravitational constant, J. Cosmol. Astropart. Phys. 03 (2010) 031, arXiv:0912.0923.
[28] S.M.R. Micheletti, Observational constraints on holographic tachyonic dark energy in interaction with dark matter, J. Cosmol. Astropart. Phys. 05 (2010) 009, arXiv:0912.3992.
[29] Y.-g. Gong, Extended holographic dark energy, Phys. Rev. D 70 (2004) 064029, arXiv:hep-th/0404030.
[30] E.N. Saridakis, Restoring holographic dark energy in brane cosmology, Phys. Lett. B 660 (2008) 138, arXiv:0712.2228.
[31] M.R. Setare, E.C. Vagenas, The cosmological dynamics of interacting holographic dark energy model, Int. J. Mod. Phys. D 18 (2009) 147, arXiv:0704.2070.
[32] R.-G. Cai, A dark energy model characterized by the age of the universe, Phys. Lett. B 657 (2007) 228, arXiv:0707.4049.
[33] M.R. Setare, E.C. Vagenas, Thermodynamical interpretation of the interacting holographic dark energy model in a non-flat universe, Phys. Lett. B 666 (2008) 111, arXiv:0801.4478.
[34] E.N. Saridakis, Holographic dark energy in braneworld models with a Gauss-Bonnet term in the bulk. Interacting behavior and the w =-1 crossing, Phys. Lett. B 661 (2008) 335, arXiv:0712.3806.
[35] M. Jamil, E.N. Saridakis, M.R. Setare, Holographic dark energy with varying gravitational constant, Phys. Lett. B 679 (2009) 172, arXiv:0906.2847.
[36] Y. Gong, T. Li, A modified holographic dark energy model with infrared infinite extra dimension(s), Phys. Lett. B 683 (2010) 241, arXiv:0907.0860.
[37] M. Suwa, T. Nihei, Observational constraints on the interacting Ricci dark energy model, Phys. Rev. D 81 (2010) 023519, arXiv:0911.4810.
[38] M. Bouhmadi-Lopez, A. Errahmani, T. Ouali, The cosmology of an holographic induced gravity model with curvature effects, Phys. Rev. D 84 (2011) 083508, arXiv:1104.1181.
[39] M. Malekjani, Generalized holographic dark energy model described at the Hubble length, Astrophys. Space Sci. 347 (2013) 405, arXiv:1209.5512.
[40] M. Khurshudyan, J. Sadeghi, R. Myrzakulov, A. Pasqua, H. Farahani, Interacting quintessence dark energy models in Lyra manifold, Adv. High Energy Phys. 2014 (2014) 878092, arXiv:1404.2141.
[41] R.C.G. Landim, Holographic dark energy from minimal supergravity, Int. J. Mod. Phys. D 25 (2016) 1650050, arXiv:1508.07248.
[42] A. Pasqua, S. Chattopadhyay, R. Myrzakulov, Power-law entropy-corrected holographic dark energy in Hořava-Lifshitz cosmology with Granda-Oliveros cut-off, Eur. Phys. J. Plus 131 (2016) 408, arXiv:1511.00611.
[43] A. Jawad, N. Azhar, S. Rani, Entropy corrected holographic dark energy models in modified gravity, Int. J. Mod. Phys. D 26 (2016) 1750040.
[44] B. Pourhassan, A. Bonilla, M. Faizal, E.M.C. Abreu, Holographic dark energy from fluid/gravity duality constraint by cosmological observations, Phys. Dark Universe 20 (2018) 41, arXiv:1704.03281.
[45] E.N. Saridakis, Ricci-Gauss-Bonnet holographic dark energy, Phys. Rev. D 97 (2018) 064035, arXiv:1707.09331.
[46] S. Nojiri, S.D. Odintsov, Covariant generalized holographic dark energy and accelerating universe, Eur. Phys. J. C 77 (2017) 528, arXiv:1703.06372.
[47] A. Oliveros, M.A. Acero, Inflation driven by a holographic energy density, Europhys. Lett. 128 (2019) 59001, arXiv:1911.04482.
[48] S. Nojiri, S.D. Odintsov, E.N. Saridakis, Holographic inflation, Phys. Lett. B 797 (2019) 134829, arXiv:1904.01345.
[49] C. Kritpetch, C. Muhammad, B. Gumjudpai, Holographic dark energy with non-minimal derivative coupling to gravity effects, Phys. Dark Universe 30 (2020) 100712, arXiv:2004.06214.
[50] M.P. Dabrowski, V. Salzano, Geometrical observational bounds on a fractal horizon holographic dark energy, Phys. Rev. D 102 (2020) 064047, arXiv:2009.08306.
[51] W.J.C. da Silva, R. Silva, Cosmological perturbations in the Tsallis holographic dark energy scenarios, Eur. Phys. J. Plus 136 (2021) 543, arXiv:2011.09520.
[52] S. Bhattacharjee, Growth rate and configurational entropy in Tsallis holographic dark energy, Eur. Phys. J. C 81 (2021) 217, arXiv:2011.13135.
[53] C. Lin, An effective field theory of holographic dark energy, arXiv:2101.08092.
[54] E.O. Colgáin, M.M. Sheikh-Jabbari, A critique of holographic dark energy, Class. Quantum Gravity 38 (2021) 177001, arXiv:2102.09816.
[55] H. Hossienkhani, N. Azimi, H. Yousefi, Constraints on the Ricci dark energy cosmologies in Bianchi type I model, Int. J. Geom. Methods Mod. Phys. 18 (2021) 2150095.
[56] S. Nojiri, S.D. Odintsov, T. Paul, Different faces of generalized holographic dark energy, Symmetry 13 (2021) 928, arXiv:2105.08438.
[57] S.H. Shekh, Models of holographic dark energy in $f(Q)$ gravity, Phys. Dark Universe 33 (2021) 100850.
[58] S. Maity, P. Rudra, Inflation driven by Barrow holographic dark energy, J. Hologr. Appl. Phys. 2 (2022) 1, arXiv:2202.08160.
[59] A. Lymperis, Holographic dark energy through loop quantum gravity inspired entropy, arXiv:2310.01050.
[60] A.Y. Shaikh, Panorama behaviors of general relativistic hydrodynamics and holographic dark energy in f(R,T) gravity, New Astron. 91 (2022) 101676.
[61] C. Tsallis, Possible generalization of Boltzmann-Gibbs statistics, J. Stat. Phys. 52 (1988) 479.
[62] J.D. Barrow, The area of a rough black hole, Phys. Lett. B 808 (2020) 135643, arXiv:2004.09444.
[63] G. Kaniadakis, Statistical mechanics in the context of special relativity, Phys. Rev. E 66 (2002) 056125, arXiv:cond-mat/0210467.
[64] G. Kaniadakis, Statistical mechanics in the context of special relativity. II, Phys. Rev. E 72 (2005) 036108, arXiv:cond-mat/0507311.
[65] S. Das, S. Shankaranarayanan, S. Sur, Power-law corrections to entanglement entropy of black holes, Phys. Rev. D 77 (2008) 064013, arXiv:0705.2070.
[66] N. Radicella, D. Pavon, The generalized second law in universes with quantum corrected entropy relations, Phys. Lett. B 691 (2010) 121, arXiv:1006.3745.
[67] E.N. Saridakis, K. Bamba, R. Myrzakulov, F.K. Anagnostopoulos, Holographic dark energy through Tsallis entropy, J. Cosmol. Astropart. Phys. 12 (2018) 012, arXiv:1806.01301.
[68] E. Sadri, Observational constraints on interacting Tsallis holographic dark energy models, Eur. Phys. J. C 79 (2019) 762, arXiv:1905.11210.
[69] E.N. Saridakis, Barrow holographic dark energy, Phys. Rev. D 102 (2020) 123525, arXiv:2005.04115.
[70] E.N. Saridakis, S. Basilakos, The generalized second law of thermodynamics with Barrow entropy, Eur. Phys. J. C 81 (2021) 644, arXiv:2005.08258.
[71] P. Adhikary, S. Das, S. Basilakos, E.N. Saridakis, Barrow holographic dark energy in a nonflat universe, Phys. Rev. D 104 (2021) 123519, arXiv:2104.13118.
[72] N. Drepanou, A. Lymperis, E.N. Saridakis, K. Yesmakhanova, Kaniadakis holographic dark energy and cosmology, Eur. Phys. J. C 82 (2022) 449, arXiv:2109.09181.
[73] A. Hernández-Almada, G. Leon, J. Magaña, M.A. García-Aspeitia, V. Motta, E.N. Saridakis, et al., Kaniadakis-holographic dark energy: observational constraints and global dynamics, Mon. Not. R. Astron. Soc. 511 (2022) 4147, arXiv:2111.00558.
[74] E.C. Telali, E.N. Saridakis, Power-law holographic dark energy and cosmology, Eur. Phys. J. C 82 (2022) 466, arXiv:2112.06821.
[75] S. Nojiri, S.D. Odintsov, E.N. Saridakis, Modified cosmology from extended entropy with varying exponent, Eur. Phys. J. C 79 (2019) 242, arXiv:1903.03098.
[76] F.K. Anagnostopoulos, S. Basilakos, E.N. Saridakis, Observational constraints on Barrow holographic dark energy, Eur. Phys. J. C 80 (2020) 826, arXiv:2005.10302.
[77] S. Nojiri, S.D. Odintsov, T. Paul, Barrow entropic dark energy: a member of generalized holographic dark energy family, Phys. Lett. B 825 (2022) 136844, arXiv:2112.10159.
[78] S. Srivastava, U.K. Sharma, Barrow holographic dark energy with Hubble horizon as IR cutoff, Int. J. Geom. Methods Mod. Phys. 18 (2021) 2150014, arXiv:2010.09439.
[79] A.A. Mamon, A. Paliathanasis, S. Saha, Dynamics of an interacting Barrow holographic dark energy model and its thermodynamic implications, Eur. Phys. J. Plus 136 (2021) 134, arXiv:2007.16020.

[80] G. Chakraborty, S. Chattopadhyay, E. Güdekli, I. Radinschi, Thermodynamics of Barrow holographic dark energy with specific cut-off, Symmetry 13 (2021) 562.
[81] Q. Huang, H. Huang, B. Xu, F. Tu, J. Chen, Dynamical analysis and statefinder of Barrow holographic dark energy, Eur. Phys. J. C 81 (2021) 686, arXiv:2201.11414.
[82] G.G. Luciano, Cosmic evolution and thermal stability of Barrow holographic dark energy in a nonflat Friedmann-Robertson-Walker universe, Phys. Rev. D 106 (2022) 083530, arXiv:2210.06320.
[83] G.G. Luciano, J. Giné, Generalized interacting Barrow holographic dark energy: cosmological predictions and thermodynamic considerations, Phys. Dark Universe 41 (2023) 101256, arXiv:2210.09755.
[84] S. Rani, N. Azhar, Braneworld inspires cosmological implications of Barrow holographic dark energy, Universe 7 (2021) 268.
[85] G.G. Luciano, Saez–Ballester gravity in Kantowski–Sachs universe: a new reconstruction paradigm for Barrow holographic dark energy, Phys. Dark Universe 41 (2023) 101237, arXiv:2301.12488.
[86] A. Oliveros, M.A. Sabogal, M.A. Acero, Barrow holographic dark energy with Granda–Oliveros cutoff, Eur. Phys. J. Plus 137 (2022) 783, arXiv:2203.14464.
[87] G.G. Luciano, Y. Liu, Lagrangian reconstruction of Barrow holographic dark energy in interacting tachyon model, Symmetry 15 (2023) 1129, arXiv:2205.13458.
[88] B.C. Paul, B.C. Roy, A. Saha, Bianchi-I anisotropic universe with Barrow holographic dark energy, Eur. Phys. J. C 82 (2022) 76.
[89] A. Jawad, S. Rani, S. Ashraf, N. Azhar, Barrow holographic dark energy in deformed Hořava–Lifshitz gravity, Int. J. Geom. Methods Mod. Phys. 19 (2022) 2250112.
[90] N. Boulkaboul, Baryogenesis triggered by Barrow holographic dark energy coupling, Phys. Dark Universe 40 (2023) 101205.
[91] A. Sheykhi, M.S. Hamedan, Holographic dark energy in modified Barrow cosmology, Entropy 25 (2023) 569, arXiv:2211.00088.
[92] W. Feng, W. Yang, B. Jiang, Y. Wang, T. Han, Y. Wu, Theoretical analysis on the Barrow holographic dark energy in the Finsler–Randers cosmology, Int. J. Mod. Phys. D 32 (2023) 2350029.
[93] Planck collaboration, N. Aghanim, et al., Planck 2018 results. VI. Cosmological parameters, Astron. Astrophys. 641 (2020) A6, arXiv:1807.06209.
[94] M. Chevallier, D. Polarski, Accelerating universes with scaling dark matter, Int. J. Mod. Phys. D 10 (2001) 213, arXiv:gr-qc/0009008.
[95] E.V. Linder, Exploring the expansion history of the universe, Phys. Rev. Lett. 90 (2003) 091301, arXiv:astro-ph/0208512.
[96] Pan-STARRS1 collaboration, D.M. Scolnic, et al., The complete light-curve sample of spectroscopically confirmed SNe Ia from Pan-STARRS1 and cosmological constraints from the combined pantheon sample, Astrophys. J. 859 (2018) 101, arXiv:1710.00845.
[97] H. Yu, B. Ratra, F.-Y. Wang, Hubble parameter and baryon acoustic oscillation measurement constraints on the Hubble constant, the deviation from the spatially flat ΛCDM model, the deceleration–acceleration transition redshift, and spatial curvature, Astrophys. J. 856 (2018) 3, arXiv:1711.03437.
[98] S. Pan, E.N. Saridakis, W. Yang, Observational constraints on oscillating dark-energy parametrizations, Phys. Rev. D 98 (2018) 063510, arXiv:1712.05746.